Baby schema modulates the brain reward system in nulliparous women

Melanie L. Glocker[a,b,1], Daniel D. Langleben[c,d], Kosha Ruparel[a], James W. Loughead[a], Jeffrey N. Valdez[a], Mark D. Griffin[a], Norbert Sachser[b], and Ruben C. Gur[a,d]

[a]Brain Behavior Laboratory and [c]Center for Studies of Addictions, Department of Psychiatry, University of Pennsylvania, Philadelphia, PA 19104; [b]Department of Behavioral Biology, University of Muenster, 48149 Muenster, Germany; and [d]Philadelphia Veterans Administration Medical Center, Philadelphia, PA 19104

Edited by Marcus E. Raichle, Washington University School of Medicine, St. Louis, MO, and approved April 10, 2009 (received for review November 17, 2008)

Ethologist Konrad Lorenz defined the baby schema (''Kindchenschema'') as a set of infantile physical features, such as round face and big eyes, that is perceived as cute and motivates caretaking behavior in the human, with the evolutionary function of enhancing offspring survival. The neural basis of this fundamental altruistic instinct is not well understood. Prior studies reported a pattern of brain response to pictures of children, but did not dissociate the brain response to baby schema from the response to children. Using functional magnetic resonance imaging and controlled manipulation of the baby schema in infant faces, we found that baby schema activates the nucleus accumbens, a key structure of the mesocorticolimbic system mediating reward processing and appetitive motivation, in nulliparous women. Our findings suggest that engagement of the mesocorticolimbic system is the neurophysiologic mechanism by which baby schema promotes human caregiving, regardless of kinship.

caregiving | functional MRI | social cognition | infant | accumbens

Ethologist Konrad Lorenz defined the baby schema (''Kindchenschema'') as a set of infantile physical features, such as large head, big eyes, high and protruding forehead, chubby cheeks, small nose and mouth, short and thick extremities, and plump body shape, that is perceived as cute and motivates caretaking behavior in the human (1, 2). In a species whose young depend on care, such bias could be evolutionary adaptive and enhance offspring survival (3–5). The behavioral effects of the baby schema have been experimentally confirmed (6–14), with implications for infant-caretaker interactions (15, 16). In ethological terms, baby schema is classified as a ''releaser'' (or ''key stimulus'' in the context of social communication), which is defined as a set of specific stimulus features sufficient to selectively elicit a particular pattern of behavior (2, 17). This abstract concept accounts for the generalization of the human response to baby schema: We not only respond positively to infants, but also to the baby schema features in adults (18), animals (12, 19), and even objects (20). Additional support for the motivating force of the baby schema comes from film, toy, and advertisement industries who capitalize on our nurturing reaction [i.e., Walt Disney's Mickey Mouse (21)].

Although the baby schema response is a fundamental social instinct that may be at the basis of human caregiving and altruism (22), its underlying neural mechanism is not well understood. Ethologists postulate that a releaser unlocks a hypothetical neurophysiologic ''releasing mechanism'' to trigger the respective behavioral response (2, 17), providing an early articulation of a putative brain-behavior relationship for the baby schema. Imaging studies demonstrated a differential brain response to child faces when compared to adult faces, with activation in multiple brain regions, including reward-related areas, such as the orbitofrontal cortex (23, 24). Together with the behavioral studies on the motivating effects of the baby schema (7, 8, 10), these findings suggest that the mesocorticolimbic system underlying reward processing and appetitive motivation may mediate the baby schema response. However, the baby schema is an abstract concept of infantile features that is distinct from children as a semantic category (1, 2). Previous studies reported a pattern of brain response to pictures of children (23, 24), but they did not dissociate the response to baby schema from the response to children. We used functional MRI (fMRI) and controlled manipulation of baby schema in infant faces to test the hypothesis that baby schema activates the mesocorticolimbic system, comprised of the dopaminergic midbrain, nucleus accumbens, amygdala, and ventromedial prefrontal cortex (25).

The majority of baby schema features are in the head and the face and most prior research has focused on these infant characteristics (6, 7, 9, 11–13). Using anthropometric (26) and morphing techniques, we manipulated photographs of 17 infants [originals courtesy Katherine Karraker, West Virginia University; (11)] to produce high (round face, high forehead, big eyes, small nose and mouth), low (narrow face, low forehead, small eyes, big nose and mouth), and unmanipulated baby schema portraits of each infant (Fig. 1). We previously demonstrated in a sample of 122 undergraduate students that the high baby schema infants are perceived as cuter and elicit stronger motivation for caretaking than the unmanipulated and the low baby schema infants (10). In the present study, 16 nulliparous female participants viewed a pseudorandom sequence of these infant faces while we measured their brain activity with event-related blood oxygenation level-dependent (BOLD) fMRI at high field (3 Tesla). During the session, participants rated the pictures for cuteness (1 = ''not very cute,'' 2 = ''cute,'' 3 = ''very cute'') with a button press on a fiber-optic response pad (FORP Current Design, Inc.).

Results

Repeated-measures ANOVA revealed a significant main effect of baby schema on participants' cuteness ratings ($F_{(2, 14)} = 60.00$, $P < 0.001$). The high baby schema infants were rated as cuter than the unmanipulated and the low baby schema infants (Bonferroni corrected pair-wise comparisons: high vs. low $P < 0.001$, high vs. unmanipulated $P < 0.001$, unmanipulated vs. low $P < 0.001$), confirming the behavioral validity of our paradigm (10).

Neuroimaging results showed that infant faces (versus crosshair) across baby schema levels activated the fusiform gyrus, thalamus, cingulate gyrus, insula, and orbitofrontal cortex (see Table 1 for a complete list of regions), in agreement with previous reports on the perception of children's faces (23, 24, 27–29). A whole-brain voxel-wise test of linear increase in BOLD fMRI signal with increased baby schema revealed significant

Author contributions: M.L.G., D.D.L., K.R., J.W.L., N.S., and R.C.G. designed research; M.L.G., J.W.L., and J.N.V. performed research; M.L.G., K.R., J.W.L., and M.D.G. analyzed data; and M.L.G., D.D.L., K.R., J.W.L., N.S., and R.C.G. wrote the paper.

The authors declare no conflict of interest.

This article is a PNAS Direct Submission.

[1]To whom correspondence should be addressed. E-mail: melanieglocker@aol.com.

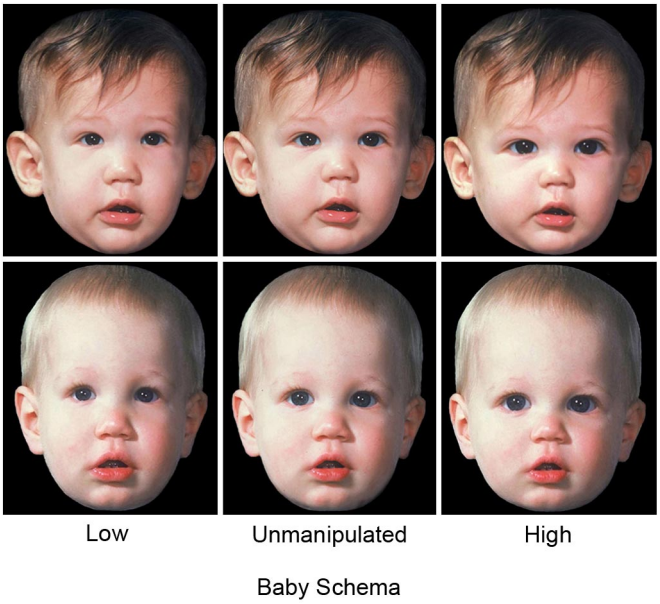

Fig. 1. Examples of low (narrow face, low forehead, small eyes, big nose and mouth), unmanipulated, and high (round face, high forehead, big eyes, small nose and mouth) baby schema faces. (Modified from ref. 10, copyright Blackwell Verlag GmbH.)

clusters of activation in 4 brain regions: the right nucleus accumbens (10, 12, −8), left anterior cingulate cortex (−4, 24, 38), left precuneus (−24, −68, 30), and left fusiform gyrus (−42, −62, −9 and −32, −52, −14; z threshold = 3.1, cluster probability $P < 0.001$) (Fig. 2*A*). A test for quadratic effects did not reveal differences between the manipulated and unmanipulated faces, ruling out any potential confound of the manipulation procedure itself.

To further probe our finding in the mesocorticolimbic system, we extracted the mean BOLD percent signal change from the activated cluster in the nucleus accumbens, which was significantly higher for high baby schema compared to unmanipulated and low baby schema infants (repeated-measures ANOVA $F_{(2, 14)} = 12.96$, $P < 0.001$; Bonferroni corrected pair-wise comparisons: high vs. low $P < 0.001$, high vs. unmanipulated $P < 0.05$, unmanipulated vs. low ns) (Fig. 2*B*).

A psychophysiological interactions (PPI) analysis showed that signal in the bilateral nucleus accumbens (left, z = 4.98, −8, 12, −8; right, z = 4.67, 10, 12, −8) covaried with the signal in the left fusiform gyrus within the context of increasing baby schema ($P < 0.0001$, uncorrected) (Fig. 3). There was no covariation in the precuneus and anterior cingulate regions.

Discussion

Our results are unique in experimental demonstration that baby schema modulates the mesocorticolimbic system. These findings suggest a neurophysiologic mechanism by which baby schema could promote human caregiving. The nucleus accumbens is a key structure of the mesocorticolimbic system that is linked to the anticipation of reward (25, 30, 31). Its activation suggests that baby schema is a positive incentive that provides motivational drive to caretaking behavior (10). By activating the nucleus accumbens, baby schema could release approach behavior toward infants (32, 33), which may reflect the urge to hold and cuddle an infant, as described by Lorenz (1, 2). The striatum, of which nucleus accumbens is part, has also been associated with more complex altruistic and affiliative processes, such as mutual cooperation (34), charitable donation (35, 36), and social bonding (27, 29). The anterior cingulate cortex projects onto the nucleus accumbens and is activated during reward-based decision making (37, 38).

Activation of the precuneus, an area associated with attention (39), suggests that baby schema allocates increased attention resources to infant faces, which might be reflected in the attention-capturing effects of infant faces in behavioral tasks (40). The fusiform gyrus is important to face perception (41, 42), with a particular role in processing invariant facial features (43). The fusiform gyrus may perceptually encode baby schema features in a face and forward this information to the nucleus accumbens for assignment of motivational value (33, 44). Support for this conclusion comes from our finding of covariation of the BOLD fMRI signal between the fusiform gyrus and nucleus accumbens. This is consistent with an emerging role of the fusiform gyrus as a major entry node in the ventrally located extended limbic and prefrontal face network (45–47). The more dorsally located precuneus and anterior cingulate cortex may also receive input from visual areas other than the fusiform gyrus, such as the inferior occipital gyri or superior temporal sulcus (45). This may explain why we did not observe signal covariation between the fusiform gyrus and precuneus or anterior cingulate regions.

From an evolutionary perspective, recruitment of "hardwired" motivational brain mechanisms in response to baby schema in nonparents could be adaptive, as human ancestors likely evolved as cooperative breeders, a social system characterized by the spread of the caretaker role to group members other than the mother (5). By engaging the mesocorticolimbic system, baby schema could motivate caring for any infant by any potential caregiver in a group, regardless of kinship. Our study cannot determine to what extent the baby schema response is an evolutionary-selected mechanism brought about by natural selection, and the extent to which it is modulated by cultural contributions. There is evidence that responsiveness to baby schema occurs in children (48) as young as 4 months of age (49), suggesting an evolutionary-shaped basis. However, responsiveness to infants is also modulated by experience and learning (50–52). Such experiences, including exposure to media and cultural artifacts in the toy industry, may therefore also modulate the individual reaction to baby schema.

Our study was limited to nulliparous women and the brain response to baby schema in men, or women in other phases of the life cycle, may differ. Some fMRI studies on the perception of nonvisual infantile cues, such as vocalization, demonstrated sex-dependent activation patterns in brain regions associated with emotion and motivation (i.e., amygdala and anterior cingulate cortex) (53, 54). Behavioral studies produced inconclusive results (7, 8, 10–14), but when sex differences were found, women were usually more responsive to baby schema than men (7, 8, 10, 12). We recently found that baby schema in infant faces induces stronger motivation for caretaking in women (10). This would suggest a stronger mesocorticolimbic response in women, who are the primary caregivers in most societies (4). However, in the same study, there were no sex differences in the perception of cuteness (10), suggesting that men and women may process baby schema similarly.

Our findings may have also been influenced by perceptual attributions to the baby schema other than cuteness (1, 2). For example, in infants attractiveness and cuteness ratings are highly correlated (55), and attractive infants are rated as more smart, likeable, healthy, friendly, and cheerful (55, 56), effects that may themselves be mediated by the baby schema. It is possible that these attributions covaried with our manipulations of baby schema in infant faces, contributing to the observed brain response. While examining the perceptual consequences of the baby schema in infant faces other than cuteness perception is outside the realm of this study, this idea could be an interesting topic for future research.

Table 1. Maximally activated voxels in brain regions that respond to infant faces versus crosshair across baby schema levels (task-related activation)

Hem	Volume[a]	Global maxima location	Local maxima location	Coordinates[b]	Z value
L	2,530	Thalamus (medial dorsal nucleus)		−6, −15, 8	14
L			Midbrain/red nucleus	−2, −27, −2	11.2
L			Thalamus (ventral lateral nucleus)	−14, −11, 8	13.1
L			Caudate head	−10, 12, −2	12.7
L			Lateral geniculate body	−24, −25, −4	12.6
R			Midbrain/red nucleus	2, −28, −2	11.2
L	632	Insula (BA 13)		−34, 16, −1	13.3
L			Superior temporal gyrus (BA 22)	−48, 9, −7	9.5
L			Claustrum	−30, 19, −1	9.46
L			Inferior frontal gyrus (BA 47)	−32, 19, −6	8.33
L			Inferior frontal gyrus (BA 13)	−36, 11, −12	8.06
L	869	Superior frontal gyrus (BA 6)		−2, 14, 51	10.1
R			Cingulate gyrus (BA 32)	4, 21, 38	8.08
R			Superior frontal gyrus (BA 6)	12, 14, 47	7.55
L			Anterior cingulate (BA 24)	−2, 26, 24	7.32
R	5,189	Cerebellum		4, −56, −29	9.95
L			Fusiform gyrus (BA 37)	−36, −51, −16	9.79
L			Cuneus (BA 30)	−16, −69, 9	8.78
L	73	Cingulate gyrus (BA 24)		−4, 3, 24	9.51
R			Cingulate gyrus (BA 24)	6, 1, 22	7.75
R			Anterior cingulate (BA 33)	6, 9, 22	5.05
R	1,078	Inferior frontal gyrus (BA 47)		34, 19, −6	8.59
R			Insula (BA 13)	28, 25, −3	8.21
R			Inferior frontal gyrus (BA 47)	32, 21, −3	8.15
R			Insula (BA 47)	38, 15, −6	7.67
R			Insula (BA 13)	36, 11, 20	7.45
R			Claustrum	36, 4, −5	7.33
L	240	Precuneus (BA 7)		−26, −50, 39	7.79
L			Inferior parietal lobule (BA 40)	−32, −47, 41	6.97
L			Superior parietal lobule (BA 7)	−28, −54, 39	6.79
L	265	Postcentral gyrus (BA 2)		−49, −19, 47	6.61
L			Postcentral gyrus (BA 3)	−44, −21, 45	6.36
L			Inferior parietal lobule (BA 40)	−44, −31, 40	6.18
L			Postcentral gyrus (BA 2)	−40, −25, 40	5.77
L	76	Precentral gyrus (BA 6)		−42, 0, 29	6.52
L			Inferior frontal gyrus (BA 9)	−46, 6, 33	6.41
L			Middle frontal gyrus (BA 9)	−51, 8, 36	5.08
R	77	Caudate (head)		14, 12, 3	6.36
R			Putamen	14, 13, −4	5.77
R			Lateral globus pallidius	12, 8, −4	5.51
R			Caudate head	14, 16, −1	5.33
R			Lateral globus pallidius	12, 6, 3	4.87
R	244	Precuneus (BA 7)		28, −64, 33	6.32
R			Superior parietal lobule (BA 7)	24, −62, 40	6.1
R			Inferior parietal lobule (BA 40)	36, −43, 41	5.99

[a]Volumes are given as number of active 3.0 × 3.44 × 3.44 mm voxels.
[b]Coordinates (X,Y,Z) in Talairach space.
Results are family-wise error corrected for multiple comparisons across the whole brain (spatial extent > 50 voxels).

The behavioral generalization of the baby schema response to the perception of adults, animals, and objects with baby schema features (12, 18–21) suggests that our neurophysiological findings may extend beyond the female-infant context. Involvement of the brain substrates for appetitive motivation may explain the success of high baby schema icons, such as the Teddy Bear (20) and the Volkswagen Beetle in popular culture.

In conclusion, our findings offer a previously unrecorded insight into the biological foundations of human caregiving and provide a neurobiological explanation to why we feel the urge to care for anything that resembles a baby.

Materials and Methods

Subjects were 16 nulliparous, right-handed women (14 Caucasian, 2 Asian) aged 20 to 28 years (mean, 24.2). Eleven of the subjects were taking hormonal contraceptives and 15 were single. All had experience with child care (i.e., baby sitting or having a younger sibling). Candidates with psychiatric, neurological, endocrinological, and cardiovascular disorders were excluded. The study protocol was approved by the University of Pennsylvania Institutional Review Board. All subjects gave written informed consent before participating.

fMRI task stimuli were 51 infant faces parametrically manipulated for their amount of baby schema. Using antropometric (26) and morphing techniques, we manipulated photographs of 17 Caucasian infants [8 boys and 9 girls aged 7–13 months with a neutral facial expression on black background (10, 11)] to produce high (round face, high forehead, big eyes, small nose and mouth), low (narrow face, low forehead, small eyes, big nose and mouth), and unmanipulated baby schema portraits of each infant (see Fig. 1). Techniques and procedures used to create the baby schema stimuli are reported in detail in Glocker et al. (10). Briefly, we operationalized baby schema in infant faces using facial features that comprise the baby schema (1, 2, 6, 9, 11, 13, 57): face

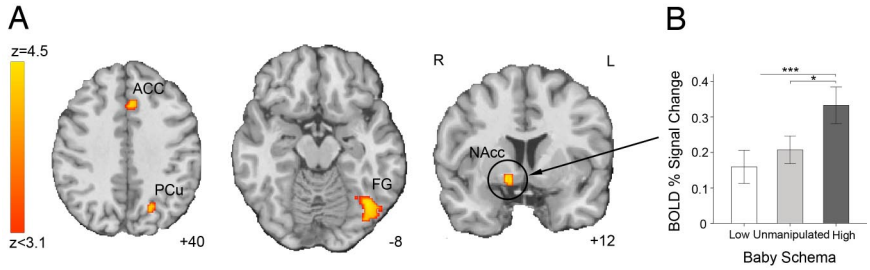

Fig. 2. Brain response to baby schema. (*A*) Linear increase in activation with increasing baby schema in the left anterior cingulate cortex (ACC; −4, 24, 38), left precuneus (PCu; −24, −68, 30), left fusiform gyrus (FG; −42, −62, −9 and −32, −52, −14) and right nucleus accumbens (NAcc; 10, 12, −8; z threshold = 3.1, cluster probability $P < 0.001$). (*B*) The mean BOLD percent signal change from baseline in the right nucleus accumbens was greatest for high baby schema, followed by the unmanipulated and low baby schema infants (repeated-measures ANOVA $F_{(2, 14)} = 12.96$, $P < 0.001$, Bonferroni corrected pair-wise comparisons $^{*}P < 0.05$ and $^{***}P = 0.001$). Error bars show SEM.

width, forehead height and eye, nose and mouth size. These features were captured by 6 facial parameters: Absolute face width (fw) in pixels with head length fixed at 500 pixels and 5 proportion indices: forehead length/face length (fol/fal); eye width/face width (ew/fw); nose length/head length (nl/hl); nose width/face width (nw/fw), and mouth width/face width (mw/fw). Using Photoshop (Adobe Systems), we measured these facial parameters in a sample of 40 unmanipulated infant photographs [20 boys and 20 girls aged 7–13 months with a neutral facial expression (10, 11)] and calculated the mean values of each facial baby schema parameter in this sample. Using morphing software (Morph Age, eX-cinder; Face Filter Studio, Reallusion Inc.), we then manipulated these facial parameters in 17 infants, randomly selected from the sample of the 40 unmanipulated infants, to produce high (fw, fol/fal, ew/fw > mean, nl/hl, nw/fw, mw/fw < mean) and low (fw, fol/fal, ew/fw < mean, nl/hl, nw/fw, mw/fw > mean) baby schema portraits of each infant. The normalized mean values (z-scores) for each facial parameter from the sample of the 40 unmanipulated infants served as a guide for our manipulations: to maintain normal facial appearance (26), the range of manipulations for each facial parameter was restricted to a z-score range of +/–2 SD. Manipulated faces were remeasured and the new facial parameter z-scores calculated. The total baby schema content within an infant's face was quantified as the average facial parameter z-score. This resulted in 17 high (mean total baby schema z-score = 1.0, SD = 0.2), 17 low (mean total baby schema z-score = –1.1, SD = 0.1), and 17 unmanipulated baby schema infant portraits (mean total baby schema z-score = 0, SD = 0.3).

During fMRI scan acquisition, participants were presented with a pseudorandom, event-related sequence (optseq2, http://surfer.nmr.mgh.harvard.edu/optseq) of the low, high, and unmanipulated baby schema faces. Each image was presented for 3 s, followed by a variable interstimulus interval (6–18 s) during which a crosshair-fixation point was displayed on a black background (total 543 s). Participants rated each face for cuteness (1 = ''not very cute,'' 2 = ''cute,'' and 3 = ''very cute'') with a button-press using a fiber-optic response pad (FORP Current Design, Inc.). No stimulus picture was presented twice. Total task duration was 11 min and 36 s.

BOLD fMRI was acquired with a Siemens Trio 3 Tesla system using a whole-brain, single-shot gradient-echo echoplanar sequence with the following parameters: repetition time/echo time = 3,000/30 ms, field of view = 220 mm, matrix = 64 × 64, slice thickness/gap = 3/0 mm, 40 slices, effective voxel resolution of 3.4 × 3.4 × 3 mm. To reduce partial voluming in orbital frontal regions, the echoplanar sequence was acquired obliquely (axial/coronal). Before time-series acquisition, a 5-min magnetization-prepared, rapid acquisition gradient-echo T1-weighted image (MPRAGE, repetition time 1,620 ms, echo time 3.87 ms, field of view 250 mm, matrix 192 × 256, effective voxel resolution of 1 × 1 × 1 mm) was collected for anatomic overlays of functional data and to aid spatial normalization to a standard atlas space (58).

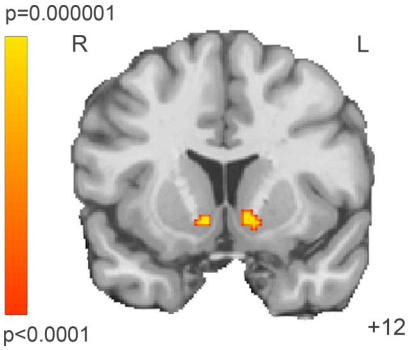

Fig. 3. PPI results showing voxels in the bilateral nucleus accumbens (left, z = 4.98, –8, 12, –8; right, z = 4.67, 10, 12, –8) that covaried with the left fusiform gyrus seed region within the context of increasing baby schema ($P < 0.0001$, uncorrected).

The fMRI data were subjected to quality control, preprocessing, and statistical analysis using FEAT (fMRI Expert Analysis Tool) version 5.63, part of FMRIB's Software Library. Subject-level preprocessing included slice-time correction, motion correction to the median image using trilinear interpolation, high-pass temporal filtering (100 s), spatial smoothing (6 mm FWHM, isotropic), and scaling using mean-based intensity normalization. The median functional image was coregistered to the corresponding high-resolution T1-weighted structural image and transformed into standard anatomical space (T1 Montreal Neurological Institute template) using trilinear interpolation. Transformation parameters were applied to statistical maps before group analyses. The brain extraction tool was used to remove nonbrain areas.

Subject-level time-series analyses were carried out using FMRIB's Improved Linear Model with local autocorrelation correction (59). Voxels showing increased BOLD signal as a function of baby schema level were tested with a parametric statistical model (60) using orthogonal basis functions up to the second order. The zero-order term modeled the mean (constant term) effect of infant faces to the crosshair irrespective of the baby schema level. The first-order term modeled a parametric linear increase in baby schema level (−1, 0, 1) and a second-order term modeled a quadratic relationship [all manipulated vs. unmanipulated baby schema (–1, 2, –1)]. The parametric model used a stepwise forward-model selection approach with 3 sequential analyses, each with the respective order terms serving as the covariates of interest. All covariates were convolved with a canonical hemodynamic response function before inclusion in the general linear model (GLM). Contrast maps of the covariates of interest were entered into a group-level 1-sample T-test. Group Z statistic maps were generated and corrected for spatial extent using Monte Carlo simulation (AFNI AlphaSim, R.W. Cox, National Institute of Health) with a minimum z threshold ≥ 3.1 and cluster probability ≤ 0.001. Identified clusters were assigned anatomic labels using the Talairach Daemon database.

To further examine our finding in the mesocorticolimbic system, we extracted the mean BOLD fMRI percent signal change from the activated cluster in the nucleus accumbens. Scaled beta coefficients (percent signal change) for the 3 baby schema levels were estimated using a second single-subject analysis. The 3 condition events (low, unmanipulated, and high baby schema) were convolved with canonical hemodynamic response function and modeled, along with their temporal derivative, in a standard GLM. Mean percent signal change values were extracted from the significant cluster in the nucleus accumbens, identified by the linear parametric model (first order) for off-line analysis and graphic presentation. A repeated-measures ANOVA, where baby schema was a within-subject factor and mean percent signal change the outcome variable, was calculated, followed by pair-wise comparisons employing Bonferroni corrections using SPSS (SPSS Inc.).

An exploratory analysis examined the physiological connectivity between the left fusiform gyrus [seed region of interest (ROI)] and the target regions identified by the first-order term of the parametric model described above (precuneus, anterior cingulate cortex, and nucleus accumbens). A whole-brain PPI analysis

was implemented in the FMRIB Software Library using procedures described by Friston et al. (61). Briefly, each subject's mean preprocessed time-series (see above) was extracted from the left fusiform gyrus region. This seed region was identified as the peak cluster in the whole-brain linear model. Similarly, target regions were identified functionally using this contrast, but at a more liberal threshold ($P < 0.01$, uncorrected) that allowed inclusion of bilateral ROIs for the precuneus, anterior cingulate cortex, and nucleus accumbens.

Subject-level PPI regressors were generated using the following design matrix: (*i*) physiological term (mean time series in the fusiform gyrus); (*ii*) psychological term (contrast vector for increasing baby schema convolved with a canonical hemodynamic response function); (*iii*) PPI term (time series $\times$ contrast vector); and (*iv*) effect of no interest regressor (unmanipulated baby schema). The model vectors were orthogonalized such that the PPI regressor did not correlate with the main effects or nuisance variables. Then, subject-specific PPI GLM models were run using the PPI regressor and movement parameters. The contrast image generated for positive PPI indicates the extent of covariation between the seed ROI (fusiform gyrus) and target brain regions within the context of the first-order term of the parametric model. Single-subject PPI images were entered into a group level, 1-sample T-test and the resulting z statistic image (Gaussianized T) was thresholded at $P < 0.0001$, uncorrected.

ACKNOWLEDGMENTS. We thank Dr. Katherine Karraker from the Department of Psychology at West Virginia University for providing the original set of infant photographs. This research was supported by a stipend of the ''Studienstiftung des deutschen Volkes'' (German National Academic Foundation) (to M.L.G.), and a grant from the Center for Functional Neuroimaging of the University of Pennsylvania and National Institute of Health Grant MH-60722 (to R.C.G.).

1. Lorenz K (1943) Innate forms of potential experience. *Z Tierpsychol* 5:235–409 (in German).
2. Lorenz K (1971) *Studies in Animal and Human Behavior* (Harvard Univ Press, Cambridge, MA).
3. Bowlby J (1969) *Attachment and Loss: Vol. 1 Attachment* (Hogarth, London).
4. Eibl-Eibesfeldt I (1989) *Human Ethology* (De Gruyter, New York).
5. Hrdy SB (2005) in *Attachment and Bonding*, eds Carter CS, et al. (MIT Press, Cambridge), pp 9–32.
6. Alley TR (1981) Head shape and the perception of cuteness. *Dev Psychol* 17:650–654.
7. Alley TR (1983) Infantile head shape as an elicitor of adult protection. *Merrill Palmer Q* 29:411–427.
8. Alley TR (1983) Growth-produced changes in body shape and size as determinants of perceived age and adult caregiving. *Child Dev* 54:241–248.
9. Brooks V, Hochberg J (1960) A psychophysical study of ''Cuteness.'' *Percept Mot Skills* 11:205.
10. Glocker ML, et al. (2009) Baby schema in infant faces induces cuteness perception and motivation for caretaking in adults. *Ethology* 115:257–263.
11. Hildebrandt KA, Fitzgerald HE (1979) Facial feature determinants of perceived infant attractiveness. *Infant Behav Dev* 2:329–339.
12. Hueckstedt B (1965) Experimental investigations on the baby schema. *Z Exp Angew Psychol* 12:421–450 (in German).
13. Sternglanz SH, Gray JL, Murakami M (1977) Adult preferences for infantile facial features: An ethological approach. *Anim Behav* 25:108–115.
14. McKelvie SJ (1993) Perceived cuteness, activity level, and gender in schematic baby-faces. *J Soc Behav Pers* 8:297–310.
15. Volk A, Quinsey VL (2002) The influence of infant facial cues on adoption preferences. *Hum Nat* 13:437–455.
16. Langlois JH, Ritter JM, Casey RJ, Sawin DB (1995) Infant attractiveness predicts maternal behaviors and attitudes. *Dev Psychol* 31:464–472.
17. Tinbergen N (1951) *The Study of Instinct* (Clarendon Press, Oxford).
18. Zebrowitz LA (1997) *Reading Faces: Window to the soul?* (Westview Press, Boulder, CO).
19. Fullard W, Reiling AM (1976) An investigation of Lorenz's ''babyness''. *Child Dev* 47:1191–1193.
20. Hinde RA, Barden LA (1985) The evolution of the teddy bear. *Anim Behav* 33:1371–1373.
21. Gould SJ (1979) Mickey Mouse meets Konrad Lorenz. *Nat Hist* 88:30–36.
22. Eibl-Eibesfeldt I (1974) *Love and Hate: The Natural History of Behavior Patterns* (Schocken, New York).
23. Leibenluft E, Gobbini MI, Harrison T, Haxby JV (2004) Mothers' neural activation in response to pictures of their children and other children. *Biol Psychiatry* 56:225–232.
24. Kringelbach ML, et al. (2008) A specific and rapid neural signature for parental instinct. *PLoS ONE* 3:e1664.
25. O'Doherty JP (2004) Reward representations and reward-related learning in the human brain: insights from neuroimaging. *Curr Opin Neurobiol* 14:769–776.
26. Farkas LG (1994) *Anthropometry of the Head and Face.* (Raven, New York).
27. Bartels A, Zeki S (2004) The neural correlates of maternal and romantic love. *Neuroimage* 21:1155–1166.
28. Nitschke JB, et al. (2004) Orbitofrontal cortex tracks positive mood in mothers viewing pictures of their newborn infants. *Neuroimage* 21:583–592.
29. Strathearn L, Li J, Fonagy P, Montague PR (2008) What's in a smile? Maternal brain responses to infant facial cues. *Pediatrics* 122:40–51.
30. Knutson B, Adams CM, Fong GW, Hommer D (2001) Anticipation of increasing monetary reward selectively recruits nucleus accumbens. *J Neurosci* 21:RC159.
31. Berns GS, McClure SM, Pagnoni G, Montague PR (2001) Predictability modulates human brain response to reward. *J Neurosci* 21:2793–2798.
32. Alcaro A, Huber R, Panksepp J (2007) Behavioral functions of the mesolimbic dopaminergic system: an affective neuroethological perspective. *Brain Res Rev* 56:283–321.
33. Panksepp J (1998) *Affective Neuroscience. The Foundations of Human and Animal Emotions* (Oxford Univ Press, New York).
34. Rilling J, et al. (2002) A neural basis for social cooperation. *Neuron* 35:395–405.
35. Harbaugh WT, Mayr U, Burghart DR (2007) Neural responses to taxation and voluntary giving reveal motives for charitable donations. *Science* 316:1622–1625.
36. Moll J, et al. (2006) Human fronto-mesolimbic networks guide decisions about charitable donation. *Proc Natl Acad Sci USA* 103:15623–15628.
37. Bush G, et al. (2002) Dorsal anterior cingulate cortex: a role in reward-based decision making. *Proc Natl Acad Sci USA* 99:523–528.
38. Rushworth MF, Behrens TE, Rudebeck PH, Walton ME (2007) Contrasting roles for cingulate and orbitofrontal cortex in decisions and social behaviour. *Trends Cogn Sci* 11:168–176.
39. Le TH, Pardo JV, Hu X (1998) 4 T-fMRI study of nonspatial shifting of selective attention: cerebellar and parietal contributions. *J Neurophysiol* 79:1535–1548.
40. Brosch T, Sander D, Scherer KR (2007) That baby caught my eye. Attention capture by infant faces. *Emotion* 7:685–689.
41. Kanwisher N, McDermott J, Chun MM (1997) The fusiform face area: a module in human extrastriate cortex specialized for face perception. *J Neurosci* 17:4302–4311.
42. Grill-Spector K, Knouf N, Kanwisher N (2004) The fusiform face area subserves face perception, not generic within-category identification. *Nat Neurosci* 7:555–562.
43. Hoffman EA, Haxby JV (2000) Distinct representations of eye gaze and identity in the distributed human neural system for face perception. *Nat Neurosci* 3:80–84.
44. Berridge KC, Robinson TE (1998) What is the role of dopamine in reward: hedonic impact, reward learning, or incentive salience? *Brain Res Brain Res Rev* 28:309–369.
45. Haxby JV, Hoffman EA, Gobbini MI (2002) Human neural systems for face recognition and social communication. *Biol Psychiatry* 51:59–67.
46. Fairhall SL, Ishai A (2007) Effective connectivity within the distributed cortical network for face perception. *Cereb Cortex* 17:2400–2406.
47. Ishai A (2008) Let's face it: it's a cortical network. *Neuroimage* 40:415–419.
48. Sanefuji W, Ohgami H, Hashiya K (2007) Development of preference for baby faces across species in humans (*Homo sapiens*). *J Ethol* 25:249–254.
49. McCall RB, Kennedy CB (1980) Attention of 4-month infants to discrepancy and babyishness. *J Exp Child Psychol* 29:189–201.
50. Frodi AM, Murray AD, Lamb ME, Steinberg J (1984) Biological and social determinants of responsiveness to infants in 10-to-15-year-old girls. *Sex Roles* 10:639–649.
51. Lovejoy MC, Graczyk PA, O'Hare E, Neuman G (2000) Maternal depression and parenting behavior: a meta-analytic review. *Clin Psychol Rev* 20:561–592.
52. Leavitt LA (1998) Mothers' sensitivity to infant signals. *Pediatrics* 102:1247–1249.
53. Seifritz E, et al. (2003) Differential sex-independent amygdala response to infant crying and laughing in parents versus nonparents. *Biol Psychiatry* 54:1367–1375.
54. Sander K, Frome Y, Scheich H (2007) FMRI activations of amygdala, cingulate cortex, and auditory cortex by infant laughing and crying. *Hum Brain Mapp* 28:1007–1022.
55. Stephan CW, Langlois JH (1984) Baby beautiful: Adult attributions of infant competence as a function of infant attractiveness. *Child Dev* 55:576–585.
56. Ritter JM, Casey RJ, Langlois JH (1991) Adults' responses to infants varying in appearance of age and attractiveness. *Child Dev* 62:68–82.
57. Enlow D (1982) *Handbook of Facial Growth* (Saunders, Philadelphia).
58. Talairch J, Tournoux P (1988) *Co-planar Stereotaxic Atlas of the Human Brain* (Thieme, New York).
59. Woolrich MW, Ripley BD, Brady M, Smith SM (2001) Temporal autocorrelation in univariate linear modeling of FMRI data. *Neuroimage* 14:1370–1386.
60. Buchel C, Holmes AP, Rees G, Friston KJ (1998) Characterizing stimulus-response functions using nonlinear regressors in parametric fMRI experiments. *Neuroimage* 8:140–148.
61. Friston KJ, et al. (1997) Psychophysiological and modulatory interactions in neuroimaging. *Neuroimage* 6:218–229.